# Winterthur/University of Delaware Program in Art Conservation

Conservation Examination Report and Treatment Proposal

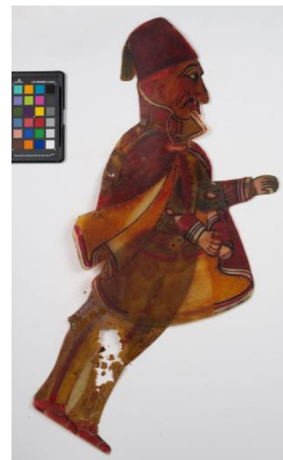

**Owner:** Winterthur/University of Delaware Program in Art Conservation (WUDPAC) Study Collection
**Accession #**: GACP 1995A
**Object:** Turkish Vizier or Pasha, Karaghiozis Greek shadow theater puppet

**Artist/Maker:** Dinos Theodoropoulos (b. 1890, d. 1975) (Gudas 1986, 141-142)
**Object Date:** 1920-1969[1]
**Materials:** Cellulose nitrate, paints/dyes (likely cellulose nitrate-based, e.g. pyroxylin), ferrous alloy
**Dimensions:** 23 11/16 x 11 5/16 x 0.05 in, 60.2 x 28.7 x 0.14 cm (H x W x thickness)

**Distinguishing Marks:** None

**Reason for Treatment:** Stabilization for storage and display.

**Examined By:** Daisy Diamond (Graduate Fellow, WUDPAC, Class of 2026)

**Consulted:** Lara Kaplan (Objects Conservator and Affiliated Assistant Professor, WUDPAC)
Lauren Fair (Conservator and Lab Head for Objects Conservation, Assistant Director of Conservation, Affiliated Associate Professor; WUDPAC)
Dr. Liora Mael (Postdoctoral Researcher, WUDPAC)
Dr. Roxanne Radpour (Assistant Professor of Imaging Science and Documentation, WUDPAC)
William Donnelly (Associate Preventive Conservator, Winterthur and Affiliated Assistant Professor, WUDPAC)

**Proposal Date:** October 14th, 2024

***A Conservation Report was completed in 2016 by Amber Kehoe, WUDPAC Class of 2019 as a first-year organic materials block documentation project (ARTC 656). Research and insights compiled by Kehoe were crucial to this report. Areas of text directly transferred from this report are indicated in italics and followed by (Kehoe 2016, page #).***

[1] This shadow puppet was recorded by the donor Mario Rinvolucri as made in the 1920s (See "Significance and Cultural Context" for additional provenance information), but evidence from consultations conducted by Amber Kehoe in 2016 with Professor of Theater Studies at Aristotle University of Thessaloniki, Dr. Anna Stavrakopoulou, and results from FTIR indicate the puppet was potentially made as late as the 1950s-1960s (1).

## Description

This cellulose nitrate shadow puppet depicts a Turkish lord (Vizier or Pasha) standing in profile and wearing a fez, red cape, and green and red attire. Dark outlines define his face, form, and clothing. The puppet is constructed of two components: an upper and lower form joined at the waist with a circular rivet to allow for hinging movement. A portion of the midsection is unpainted, indicating the upright orientation of the puppet and minimizing darkening of the design when illuminated (Pouliot 2016). Black, red, yellow, green, and possibly blue paints and/or dyes were applied to both sides of the now green-gray, semi-transparent cellulose nitrate substrate. Two circular holes likely served as sites for a rod attachment to introduce motion to the puppet. One hole is located on the proper right (PR) shoulder, and the other is located on the lower body near the central rivet. There are eight areas of historic ferrous metal repairs (see “Condition” for additional information).

## Significance and Cultural Context

The oral art of shadow theater originated in India and China in the 4th-1st century BCE. *Traditionally, the puppets were made of translucent skin or rawhide (Pouliot 2016). This art form spread to South-East Asia during the 2nd century A.D. and eventually made its way through the Middle East into Turkey by the 16th century. The sultans of the Ottoman Empire “regularly held shadow-theater performances at the ancient Hippodrome of Constantinople and provided the basic framework for what would later emerge as the Greek shadow theater” (Gudas 1986, 14-15). Shadow theater finally appeared in Greece, France, and England towards the end of the 18th century* (Kehoe 2016, 2). In Greece, the shadow plays were “performed by a single man, the *karaghiozopechtis*, who handled and impersonated all the two-dimensional puppets behind an illuminated cloth screen, the *berdés*” using candles or other sources of illumination (figs. 1-2) (Papageorgiou 2014, 80; Gudas 1986).

Figure 1. Modern shadow theater puppeteer, Vangos, and Pasha’s palace (left) behind the *berdés*. 35 mm photographic slide taken in 1969 courtesy The British Museum (Eu,F.T.6341).

Figure 2. Contemporary Karaghiozis performance. Image courtesy P. Kapetanidis (Papageorgiou 2014, 82).

The Karaghiozis (also spelled Karagiozis) tradition is named after its principal puppet character, the “clever, humpbacked fool-hero Karagiozis, who appears in many guises, surrounded by a cast of folk caricatures from all walks of life” (fig. 3) (Myrsiades and Myrsiades 1992). Karaghiozis plays were not just entertainment: the often satirical and political performances created avenues to criticize the government and circumvent censorship regulations through allegory (Myrsiades and Myrsiades 1992, 1). These plays were also evolving expressions of meaning co-created by the performer and the audience. As described by Linda and Kostas Myrsiades, the Karagiozis text “is not fixed but emerges in performance as a dynamic, ongoing process that strikes a balance between stability and instability. … [The Karaghiozis tradition], transmitted from generation to generation, consists of a balance of physical playing techniques, spontaneous improvisation, and traditional ordering" (1992, 91). Puppeteers created their own puppets, which established their own individuality while incorporating traditional patterns (Myrsiades and Myrsiades 1992, 81).

The puppet described in this report (GACP 1995) was made by Greek player Dinos Theodoropoulos, who *entered into Karaghiozis shadow theater in 1904 and became a famous player during its golden age from 1925 to 1935 (Gudas 1986, 108, 130; Stavrakopoulou 2002, 4).* In the 1930s, a significant proliferation of plays were inspired by the inventive work and significant mentorship of Theodoropoulos (Papageorgiou 2014, 101; Myrsiades and Myrsiades 1992, 103). *Similar to most Karaghiozis players, Theodoropoulos constructed and repaired his own puppets (Stavrakopoulou 2016)* (fig. 4), therefore the repairs observed on GACP 1995A were likely done by him during its active use*. Interestingly, he was responsible for "introducing gelatine*[2] *figures and the use of a microphone and record-player to the shadow theater" (Gudas 1986, 142;* Kehoe 2016, 2-3). He traveled extensively and performed across half a century, leaving an influential mark on the Karaghiozis tradition (Myrsiades and Myrsiades 1992, 103).

Figure 3. Karagiozis shadow puppet created by Eugenios Spatharis. Greece, painted hide, 1950-1978. The British Museum, UK. Eu1978,02.1.

Figure 4. Detail of shadow puppet created by Constantinos Theodoropoulos with metal repairs and patches. Greece, plastic, circa 1920. The British Museum, UK. Eu1970,01.2.

[2] *Some sources referred to Theodoropoulos' puppets as cellulose nitrate puppets while others called them gelatine (or gelatin) puppets. In a long interview with the collector Mario Rinvolucri, Theodoropoulos stated "that he made his own puppets and discovered a new material in the USA called "gelatine" that he used for his puppets" (Stavrakopoulou 2016). Perhaps people noticed that cellulose nitrate and gelatin exhibit similar characteristics and the terms were used synonymously by the Greek theater community during the mid-20th century* (Kehoe 2016, 1).

GACP 1995A depicts the Turkish Vizier in the Karaghiozis shadow puppet tradition, as rendered by Theodoropoulos. The Turkish Vizier, also called Pasha in some performances, is a wealthy, powerful, dignified, and authoritative figure. *Karaghiozis often makes fun of him by calling him "patsas", meaning tripe* (Gudas 1986, 158; Kehoe 2016, 3). GACP 1995 was donated to the WUDPAC study collection alongside three other shadow puppets in 2015 by the Mario Rinvolucri Collection of Modern Greek Shadow Plays, Milman Parry Collection of Oral Literature at Harvard University (figs. 5-7). Mario Rinvolucri acquired this puppet from Dinos Theodoropoulos in 1969.

Figure 5. Manousos, The Cretan. Dinos Theodoropoulos, collected in 1969 by Mario Rinvolucri in Greece. Image courtesy WUDPAC study collection record (GACP 1995B).

Figure 6. Manousos, The Cretan. Dinos Theodoropoulos, collected in 1969 by Mario Rinvolucri in Greece. Image courtesy WUDPAC study collection record (GACP 1995C).

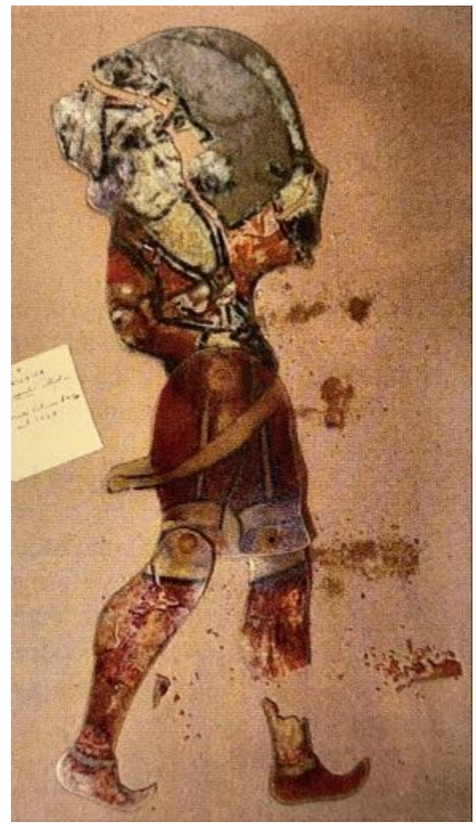

Figure 7. Turkish Soldier. Dinos Theodoropoulos, collected in 1969 by Mario Rinvolucri in Greece. Image courtesy WUDPAC study collection record (GACP 1995D).

## Materials and Manufacture

Material composition of the puppet was identified by Kehoe through technical analysis in 2016 (see Examination and Analysis for a full summary of testing and results). The substrate was determined to be cellulose nitrate.[3] Cellulose nitrate is manufactured through polymerization by soaking cellulose pulp in a mixture of nitric acid and sulfuric acid with plasticizers, including camphor,[4] and additives, including stabilizers[5] (fig. 6).

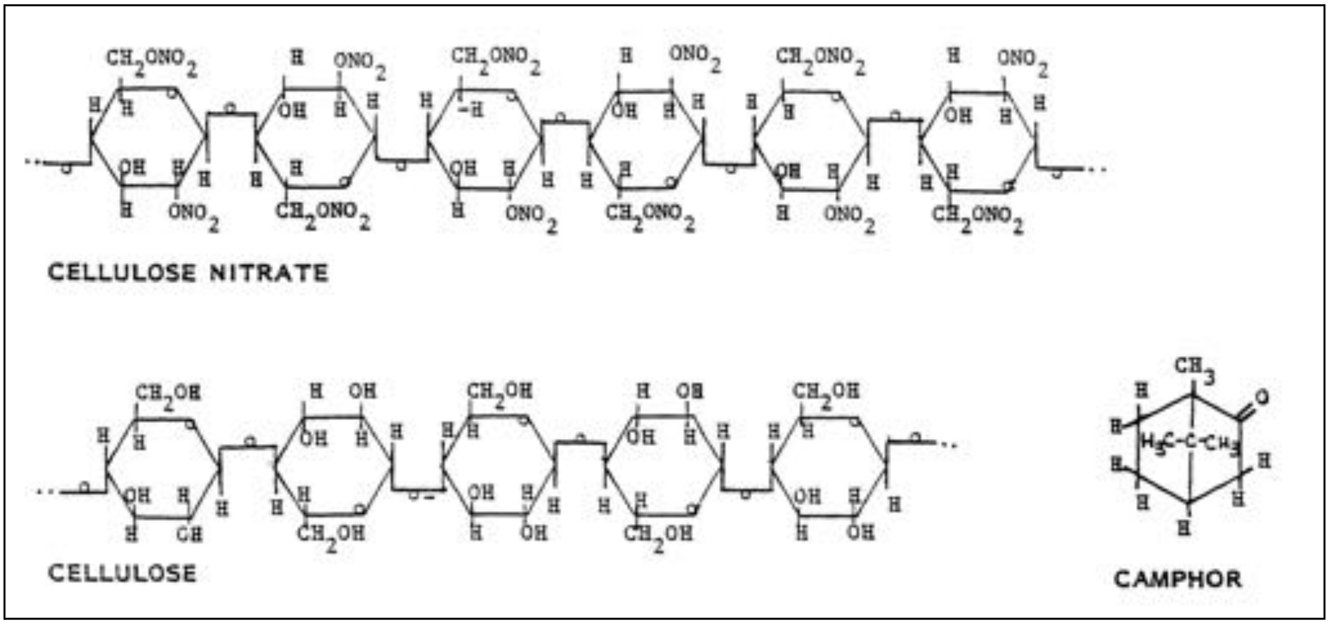


Figure 6. Cellulose nitrate, cellulose, and camphor molecules. Image courtesy Reilly 1991, 148.

To create sheets, this material would then be pressed into blocks and could be machine cut or sliced and finished with heat, pressure, or solvent (Reilly 1991, 151-153).[6] Theodoropoulos could have then sawed the puppet components from the sheet and potentially smoothed the edges with abrasive papers or solvent, painted/dyed the pieces, and joined them together with a central rivet. Based on microscopic examination, the raised substrate directly surrounding the metal repairs may indicate that the wire was heated to pierce the cellulose nitrate.

Cellulose nitrate colorants include pigments and dyes (Reilly 1991, 149). Pyroxylin lacquer is a cellulose nitrate-based finishing material that forms stable bonds with cellulose nitrate substrates and was used as a coating on wood and other thin materials. Analytical tests suggest Theodoropoulos used a cellulose nitrate-based paint/dye, potentially pyroxylin. The colorant layer does not gradually diffuse into the substrate unless it is cracked or degraded (Kehoe 2016, 3; see "Examination and Analysis" for additional information).

---

[3] Cellulose nitrate with a camphor plasticizer is sometimes generically referred to as celluloid in the literature. However, this is not to be confused with Celluloid, the trade name for a cellulose nitrate product produced in the 1870s in the United States (Coughlin 2023; Reilly 1991, 147).

[4] Camphor is a terpenoid resin from the evergreen *Cinnamomum camphora* that has excellent gelatinizing properties with a high melting point, resulting in a somewhat flexible solid at room temperature. Additionally, camphor has relatively low volatility and is resistant towards chemical agents used in the manufacturing process of cellulose nitrate (Reilly 1991, 149).

[5] Stabilizers for translucent cellulose nitrate included aryl phenyl ureas, lactates (sodium, potassium, calcium, strontium, magnesium), and more. Stabilizers for opaque cellulose nitrate included zinc oxide, which also acts as an opacifier, and zinc carbonate fillers (Reilly 1991, 150; written communication with Lara Kaplan, 9/26/2024). Some suggest that zinc oxide acts as an antioxidant to slow the rate of polymer crosslinking due to photo-oxidation (Kehoe 2016, 6; Shashoua 2008).

[6] Sheets could also be formed by solvent processing: cellulose nitrate could be dissolved in solvent (acetone, methyl ethyl ketone, etc.) and cast into molds or painted out to build up layers (Kehoe 2016, 4).

## Condition

*Overall*

This puppet is in poor and highly unstable structural condition with fair aesthetic legibility. The main condition concerns include: severe embrittlement, splits, cracks, loss in the legs, active corrosion associated with historic repairs, blooming, and overall surface grime (fig. 7). GACP 1995A is in comparatively more legible aesthetic condition than other examples of Theodoropoulos's plastic shadow puppets in the WUDPAC study collection.

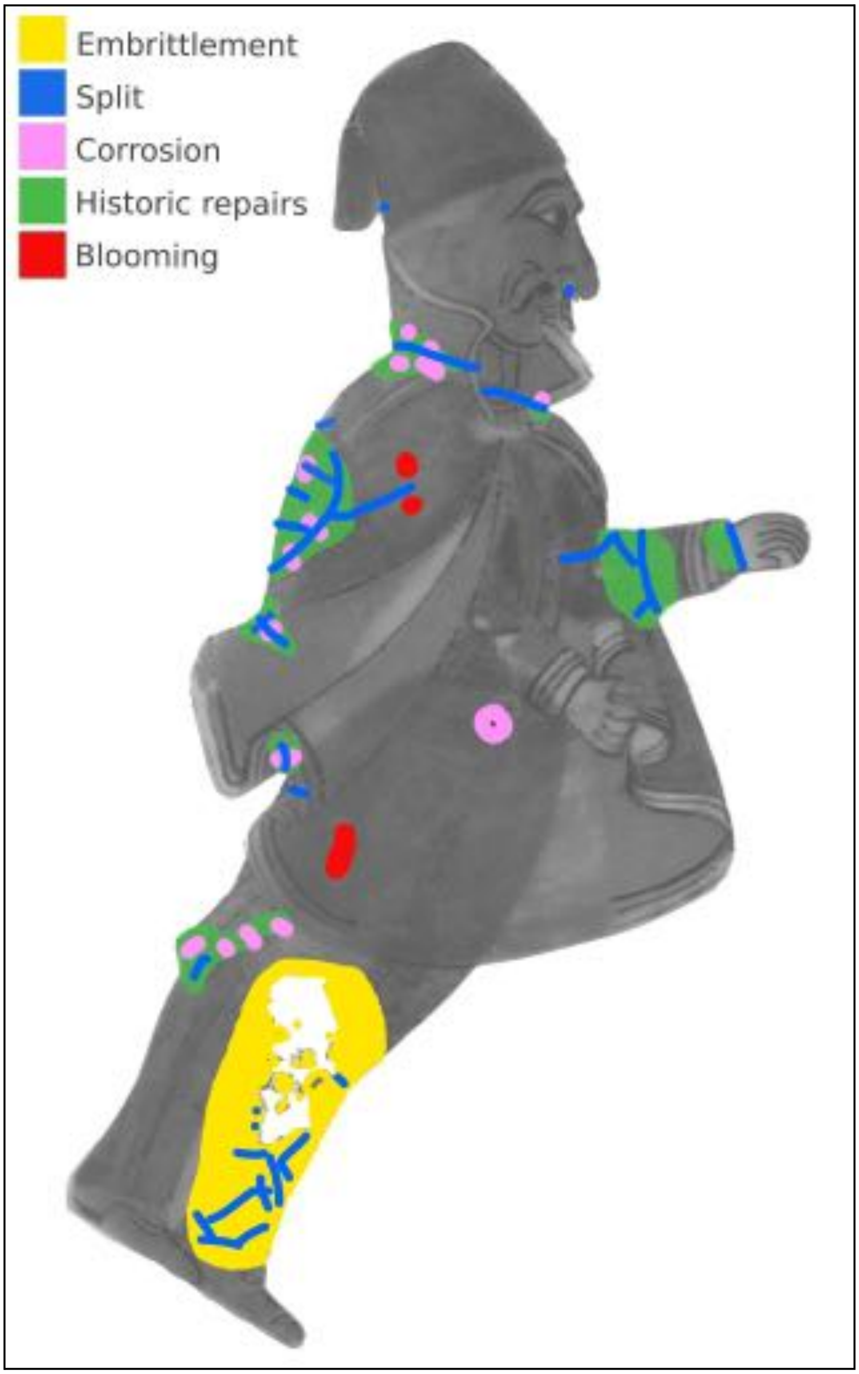


Figure 7. Condition diagram.

*Substrate*

Severe embrittlement in extensively degraded areas has led to crumbling and crizzling in a cubic degradation pattern that penetrates the internal cellulose nitrate substrate (figs. 8-10).[7] This is particularly prominent on the central third of the visible portion of the proper left (PL) leg. Splits and cracks are associated with this area of degradation ranging from 0.05 to 2.5 cm in length. This brittleness may have been caused by photo-oxidation from an illumination source directed at the lower body or a degradation reaction caused by the paint/dye and substrate interaction, as evidenced by the distinct edge of cubic crystal formation along the paint/dye edges (fig. 10). Basic pigments in cellulose nitrate lacquers may increase the rate of deterioration through alkaline hydrolysis induced nitrate loss (Reilly 1991, 154). Although much less severe than the lower body, overall embrittlement completely limits handling in the present condition. There is a loss of approximately 9 x 4 cm on the legs. Tears, cracks, and warping on the overall puppet are prominent in areas of high mechanical stress where a rod attachment was located or where the substrate was cut at an angle, rather than a curve. Additionally, the substrate has a slight planar deformation, likely due to moisture fluctuations and mechanical stresses. When the shadow puppet is on a flat surface, the warping of the lower PR side of the cape, chin, and knees of the figure lifts approximately 0.5 to 2 cm higher than the rest of the puppet. There are subtle linear, curved abrasions between the upper and lower components, likely indicative of where the materials came in contact when motion was introduced to the puppet.

Figure 8. Severe embrittlement on PL leg.

Figure 9. Micrograph, 64x magnification.

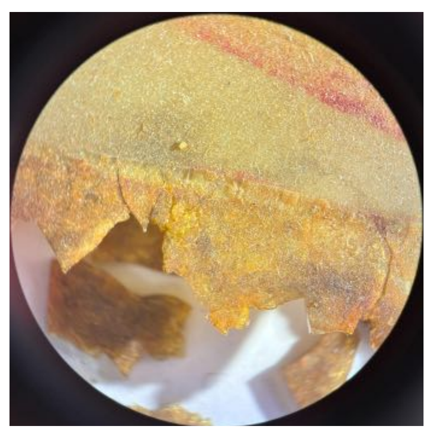

Figure 10. Micrograph illustrating potential connection to dye used (degradation aligned with color). 100x magnification.

[7] All micrographs (figs. 7-17) captured with an iPhone 15 (ISO 50-320, 26-30mm, f 1.6, 1/120-1/60s) through the eyepiece of Leica Wild M3C stereomicroscope illuminated by a Intralux 6000 light source.

*Metal repairs*

There are eight historical structural repairs utilizing ferrous wire of varying thicknesses that correspond to areas of strain (see fig. 7 for exact locations). Some repairs appear to have failed during the object's active use and additional metal wires were added, as evidenced by unused holes near remaining repairs in the PR shoulder and PL arm. Two repairs include rectangular patches, likely cellulose nitrate, for added support.

There is degradation between the active corrosion of the ferrous metal repairs and active degradation of the cellulose nitrate substrate. The cellulose nitrate has cracked near piercing sites for metal repairs. The extent to which metal cations are accelerating plastic degradation cannot be fully evaluated, as the areas in most direct contact with the metal are not visible. This corrosion has desiccated blisters and bright reddish-orange curls of corrosion product similar to those observed with chloride corrosion (figs. 9-12). However, it is unclear where chlorides would be coming from, and nitric acid accelerated corrosion is more likely. Acidic nitrogen oxides that offgas from degrading cellulose nitrate react with water to form nitric acid, which then reacts with iron to form hygroscopic iron (II) and iron (III) nitrates. Additionally, acidic pollutants can attract and trap moisture next to the metal surface and accelerate corrosion (Selwyn 2004, 104). In a research analysis of steel in contact with cellulose nitrate, "bubbles" and "elongated structures" containing a ferric nitrate and an iron hydroxy hydrate were identified in the corrosion products (de Bruyn-Ouboter and Kutzke 2024, 43).

Some corrosion likely occurred during the puppet's performance lifetime, as evidenced by repair replacements. However, it is likely these repairs have since further degraded as they are structurally unstable and detaching. Since 2016 per Kehoe's condition report, the corrosion has worsened even though the object has been stored in a relatively controlled temperature and relative humidity environment (figs. 11-16).

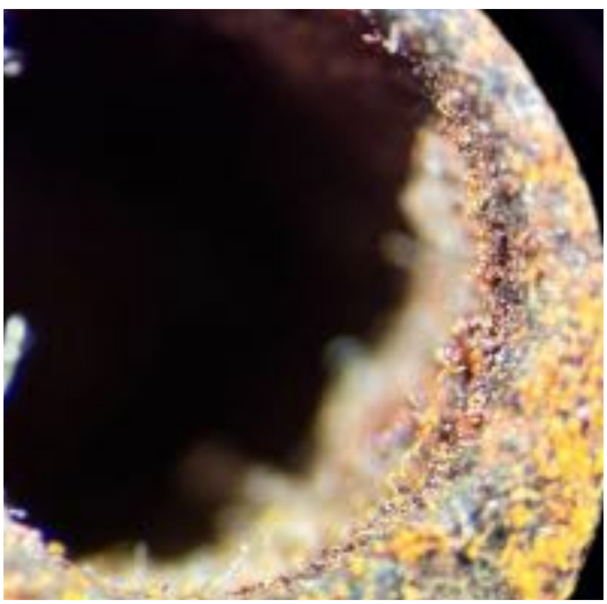

Figure 11. Desiccated blisters and corrosion product on the interior central rivet. 400x magnification.

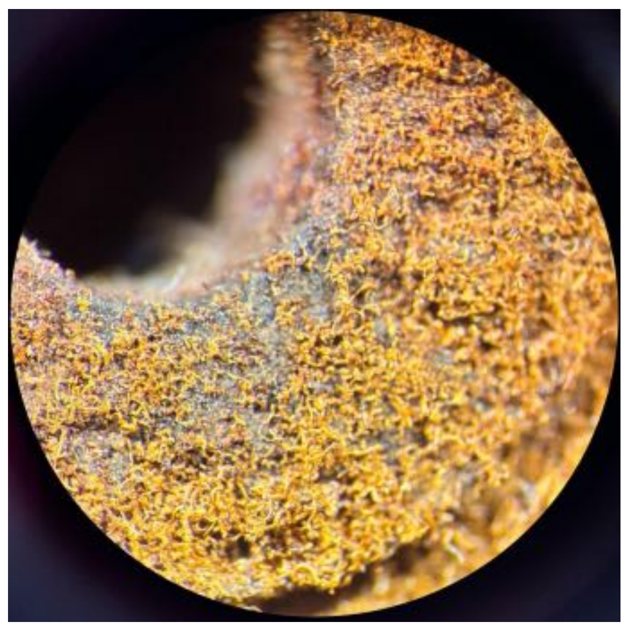

Figure 12. Desiccated blisters and corrosion product on the central rivet. 400x magnification.

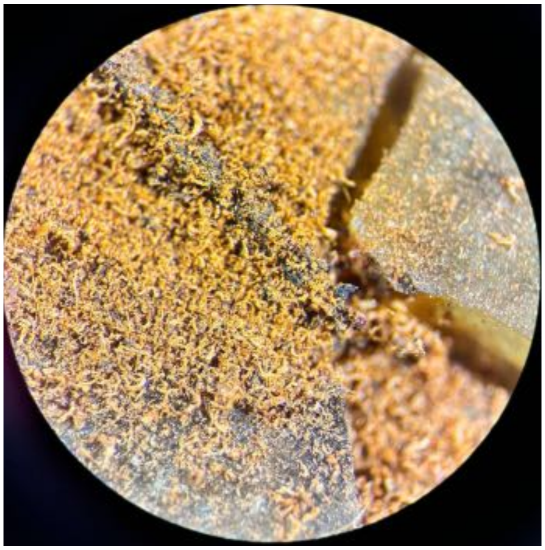

Figure 13. Desiccated blisters and corrosion product associated with the PR leg repair. 400x magnification.

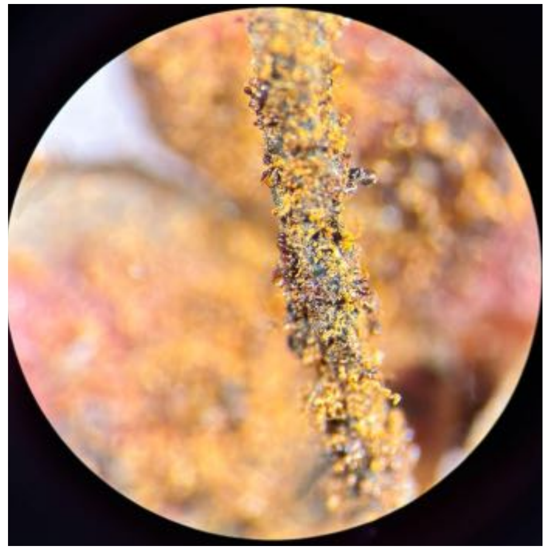

Figure 14. Desiccated blisters and corrosion product on the cape PR lower edge repair. 400x magnification.

Figure 15. Corrosion associated with historic repairs near the loss on the leg, 2016. Image courtesy Amber Kehoe.

Figure 16. Corrosion associated with historic repairs near the loss on the leg, 2024.

*Applied Color*

The color layer has minor losses due to abrasion (fig. 17) and delamination in areas of high cubic embrittlement near the loss on the leg, particularly for the red colorant (fig. 18). Additionally, the substrate has likely yellowed overall due to the development of chromophore groups with chemical degradation. Two minor areas of surface blooming are present on the upper and lower PR of the cape ranging from 0.5 to 3 cm with cubic crystals, cracking, and associated embrittlement visible under magnification (figs. 19-20). However, this embrittlement is much more structurally stable than the leg as it is surrounded by less degraded cellulose nitrate. This bloom could be caused by antioxidants or other additives from the cellulose nitrate polymeric matrix migrating to the surface (Coughlin 2023). Overall surface grime includes a white particulate with fibrous components visible in previous micrographs. There is one accretion 6 cm below the central rivet (fig. 21). The substrate has likely yellowed over time as chromophore groups developed with chemical decomposition (Coughlin 2023).

Figure 17. Abrasion to color layer near the cape, upper center buttons. 160x magnification.

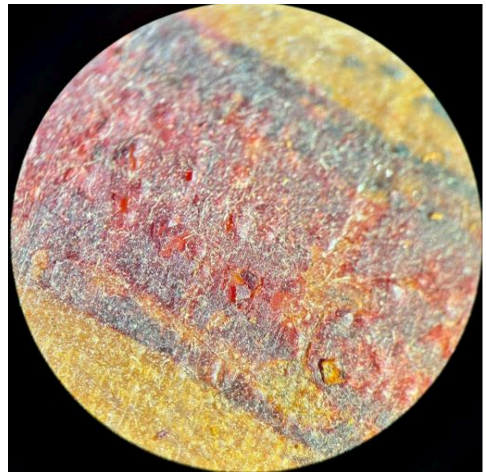

Figure 18. Delamination of color layer near the knees. 160x magnification.

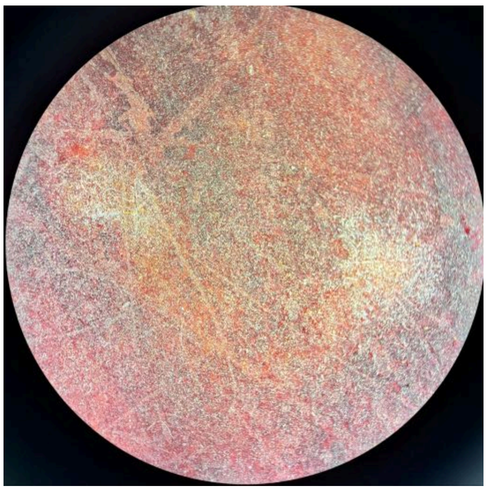

Figure 19. Blooming on the cape, upper PR. Magnification 64x.

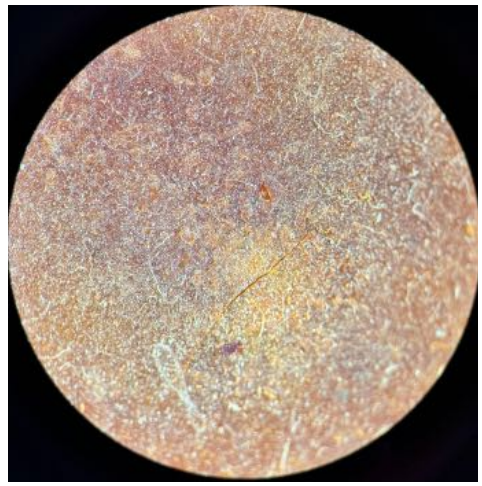

Figure 20. Embrittlement and crazing within bloom on the cape, lower PR. Magnification 160x.

Figure 21. Micrograph of surface accretion on the lower center of the cape. 160x magnification.

## Examination and Analysis

A summary of analytical analysis completed primarily in 2016 is provided (table 1). See "Appendix I. Before Treatment Photo Documentation" for technical imaging and "Appendix II. Prior Analysis" for equipment used, reference images, spectra, and tables from analytical testing and examination.

Table 1. Summary of analytical methods [N = Noninvasive, I = Invasive, Nd = Non-destructive, D = Destructive].

| Method | Goals of Testing | Results and Conclusions |
|---|---|---|
| Ultraviolet induced visible fluorescence (UVF) imaging (Diamond 2024) | Identification and spatial distribution of paints/dyes [N, Nd] | The red media has a strong bright orange fluorescence (see "Appendix I. Before Treatment Photo Documentation"), potentially indicative of a madder-based dye or pigment . |
| Visible induced visible luminescence (VIVL) imaging (Diamond 2024) | Identification and spatial distribution of pigments, in this case to confirm the presence of madder-based dyes or pigments [N, Nd] | The red media has a characteristic bright luminescence (see "Appendix I. Before Treatment Photo Documentation"), consistent with a madder-based dye or pigment. |
| Diphenylamine (DPA) microchemical spot tests[8] | Confirms cellulose nitrate in the substrate and paint/dyes by detecting the presence of nitrates [I, Nd] | There was a positive, dark blue result for the substrate and red paint/dye on the surface, suggesting that both are cellulose nitrate-based. |
| Cresol red pH indicator strips[9] | Detects volatile nitric acids resulting from volatile acidic cellulose nitrate degradation [N, Nd] | The strips did not change color after one week in 2016. Currently, the strips have very subtle and minor red in the corners after years of exposure, indicating the cellulose nitrate underwent very slight chemical degradation during the past eight years. |
| Ninhydrin microchemical spot test[10] | Evaluate potential use of gelatin in the substrate by detecting proteins [I, D][11] | A positive, pale blue result could indicate that the substrate contains proteins; however, a false positive is common. |
| Transmission-Fourier transform infrared (FTIR) spectroscopy[12] | Characterize composition of the substrate [I, D]. | The substrate contains cellulose nitrate and camphor plasticizer retained within the plastic matrix. This has potential implications for the age of the object. Proteins were not detected (See "Appendix II. Prior Analysis"). |
| X-ray fluorescence (XRF) spectroscopy[13] | Determine elemental composition of inorganic materials present [N, Nd]. | Indicates the presence of calcium (surface dirt), iron (surface dirt and historic repairs), copper (surface dirt), and zinc (potentially from the plastic formulation, i.e. zinc |

[8] Conducted by Amber Kehoe with support from Lara Kaplan in November 2016.
[9] Conducted by Amber Kehoe with support from Bruno Pouliot in November 2016.
[10] Conducted by Amber Kehoe with support from Dr. Chris Peterson in November 2016.
[11] Even though cellulose nitrate was confirmed with other analysis, testing for protein was conducted in case a gelatin component might be present.
[12] Conducted by Dr. Kristin deGhetaldi and Amber Kehoe in November 2016.
[13] Conducted by Dr. Kristin deGhetaldi and Brian Baade; interpreted by Dr. deGhetaldi, Baade, and Kehoe in November 2016.

| | | |
|---|---|---|
| | | oxide stabilizer, or surface dirt) on the object. Paints/dyes are likely of organic composition (See "Appendix II. Prior Analysis"). |
| Cross-section microscopy (CSM)[14] | Show stratigraphy of substrate layers [I, Nd] | Paint/dye visible on top and bottom of substrate layer. Non-uniform interior. (See "Appendix II. Prior Analysis"). |

## Purpose of Treatment

The purpose of this treatment is to surface clean and stabilize the shadow puppet as much as possible and provide appropriate long-term storage. Based on Kehoe's 2016 consultation, Dr. Stavrakopoulou advocated for a holistic approach to preservation to maintain all aspects as best as possible–including evidence of use, aesthetics, function, and form–even though it is unlikely the puppet will be used again in a performance context (Kehoe 2016, 7-8). The upwards-facing side of the puppet must be addressed first, as the object is too fragile in its current state to turn over.

## Treatment Proposal

1. **Carry out pre-treatment examination and photo documentation** (*completed, 3 hours*).

2. **Evaluate applicability of additional analysis and comparison to associated shadow puppets to further clarify degradation concerns and preservation approaches** (*est. 10 hours*).
    - Complete Fourier transform infrared reflectography (FTIR) to evaluate the substrate composition. Additionally, this will help determine if degradation has resulted in a chemical change in the past 5 years when compared to previous FTIR results (Kehoe 2016).
    - Revisit cross section microscopy (CSM) to determine the extent of crazing on internal and external surfaces, as well as potential layer structures.
    - Investigate corrosion composition and evaluate nitrate and/or chloride presence and source with silver nitrate spot tests or FTIR.
    - Evaluate if repairs are also cellulose nitrate with the diphenylamine spot test.

3. **Mechanically reduce corrosion products** (est. 8 hours).
    - Removal of corrosion products transferred onto the cellulose nitrate substrate could include cleaning with a soft-bristled brush into a HEPA filtered low-speed vacuum or picking up particulates with dried Lascaux® 360 on a skewer or microswab (Kim et al. 2024).
    - Reduction of corrosion on metal elements could be done under magnification using a scalpel, steel pick, or similar tool. If possible, slipping silicone release Mylar around the metal would protect the surrounding cellulose nitrate.
    - If the substrate is too fragile to clean before stabilization, proceed with step 6 prior to corrosion reduction and surface cleaning.

4. **Overall surface clean to reduce remaining corrosion products, surface grime, loose particulates, and blooming** (*est. 1 – 10 hours*).
    - Overall dry surface clean with a cosmetic sponge, soft brush, and/or HEPA filter-equipped vacuum in linear passes.
    - If overall wet cleaning is deemed necessary, complete solubility spot tests to evaluate efficacy and safety.

[14] Sample prepared and photographed by Amber Kehoe in 2016 with the guidance of Matthew Cushman.

        - Solvents tested could include: deionized water, silicone solvent D4, isopropanol, ethanol, 1:1 isopropanol and ethanol, mineral spirits with low aromaticity, and n-butanol (Kim et al. 2024; Owens 2017). Under magnification, evaluate material impacts immediately following cleaning and after 48 hours.
        - Apply the most effective and least damaging cleaning method, or combination of methods, to surface clean as possible. Continually evaluate efficacy of cleaning methods, as more severely degraded areas of cellulose nitrate have different material sensitivities (Kim et al. 2024).
    - Reduce surface blooming following testing. Methods for bloom reduction could include mechanical reduction or isopropanol applied with a fine brush (Kim et al. 2024).

5. **Evaluate methods to address active corrosion** (*est. 10 hours*).
    - Investigate varied approaches including, but not limited to: application of corrosion inhibitors (for example, tannic acid), coating of repairs, and replacement of ferrous components.
    - Ethical considerations include: reversibility as well as efficacy of interventive treatments, original artistic intent, historical significance of repairs, and the lifespan of the object.

6. **Stabilize areas of severe embrittlement and cubic crystal formation** (*est. 12 hours*).
    - Test potential consolidation methods (all solutions 1-5% w/v):
        - Aquazol 50 in isopropanol, ethanol, 1:1 isopropanol and ethanol, and deionized water
        - Paraloid B-67 in n-butanol or low aromaticity mineral spirits (Kim et al. 2024)
        - Paraloid B-72 in ethanol
    - Apply the most effective and least damaging consolidation method, or combination of methods, to stabilize the substrate in areas of cubic crystal embrittlement, as possible. Continually evaluate efficacy of stabilization, as more severely degraded areas of cellulose nitrate have different solubility parameters (Kim et al. 2024).

7. **Reattach extant fragments** (*est. 8 hours*).
    - Complete localized testing of adhesives in solutions ranging from 20-45% w/v, including the following:
        - Paraloid B-67 in n-butanol (Kim et al. 2024)
        - Aquazol 200 in isopropanol, deionized water, or a combination (Kim et al. 2024)
        - Aquazol 500 in isopropanol, deionized water, or a combination (Kim et al. 2024)
        - Paraloid B-72 in ethanol
    - Consolidate break edges with the aforementioned method from consolidation testing.
    - Apply the most effective and least damaging adhesion method, or combination of methods, to rejoin extant fragments as possible. Consider the use of a paper bridge (i.e. tengucho or kozo) to provide additional structural support. Continually evaluate efficacy of stabilization, as more severely degraded areas of cellulose nitrate have different solubility parameters (Kim et al. 2024).

8. **Fill the large loss on the leg** (*est. 5 hours*).
    - Create a toned detachable insert or cast resin fill with conservation-grade fill materials, adhesive for attachment, and colorants for aesthetic integration. Potential fill materials could include Asian paper toned with Golden Fluid Acrylics or cast and pigmented B-72. Adhesive selection will be influenced by testing in step 7.

9. **If structurally stable, turn the object over to evaluate the condition of the other side. Address condition concerns as possible** (*est. 5 hours*).

10. **Apply an accession number, if deemed necessary** (*est. 1 hour*).
    - Methods could include applying a barrier layer and writing followed by a coating or applying adhering a secondary support with a Rhoplex acrylic emulsion, Paraloid B-72 in a compatible solvent, or Jade 403 poly(vinyl acetate) emulsion (Braun 2007, 100-101).

11. **Update housing enclosure** (*est. 5 hours*).
    - Maintain ventilation of storage housing to prevent the build-up of acidic gasses. Consider the use of cresol red applied to a string to monitor the distance traveled of nitric acid off-gassing.
    - Certain malignant plastics benefit from archival corrugated board (i.e. Blueboard) as a housing material since it adsorbs acidic by-products with minimal acceleration of plasticizer leaching (Coughlin 2023). Adsorbents should not be included, as they are often ineffective or even accelerate loss of plasticizer, resulting in shrinkage (Shashoua, Schilling, and Mazurek 2014).
    - Create dimensional supports from Volara foam to reduce stress on the warped plastic.

12. **Carry out post-treatment photodocumentation and write treatment repor**t (*est. 1-4 hrs*)
    - If the puppet is stable enough to transfer onto a clear, rigid support upright, consider creating an imaging set-up similar to shadow puppet performances but horizontal to photograph its shadow (William Donnelly, personal communication, October 2nd, 2024). This could be one approach to preserve the intangible, performance quality of this Karaghiozis shadow puppet.

*Total estimated time: 68 – 80 hours.*

Daisy Diamond

**Daisy Diamond** **Date: 10/16/2024**

Conservation Graduate Fellow

Lara Kaplan

**Lara Kaplan** **Date: 10/16/2024**

Supervising Conservator

# Conservation Treatment Report

## Additional Observations

It is possible that the hand could have fallen off and was reattached at a shortened distance. The knee repair may have also come from what used to be the wrist. Under magnification, dyed cellulose nitrate "coats" some of the metal repairs, potentially indicating the metal was heated to push through the substrate. Although referred to as having a recto and verso throughout treatment documentation, it is likely that this puppet may not have been perceived by the performer or audience as having a distinct "front" or "back." The puppet was probably used on both sides, depending on the direction the character was moving or facing.

## Treatment Summary

Reduced corrosion and mechanically stabilized the embrittled substrate to the extent possible. Surface cleaned the recto and verso of the puppet. Consolidated highly degraded and structurally unstable cellulose nitrate and then stabilized with a lining on the verso. Created a fill to visually compensate for the loss. Designed and assembled a housing enclosure to maximize accessibility and support the warped substrate. Documented the shadow and created a replica to preserve the intangible qualities of the puppet.

## Treatment Steps

1. **Carried out pre-treatment examination and photo documentation** (*3 hours*).
2. **Completed additional analysis to further confirm substrate and degradation product composition** (*5 hours*).
    - **Diphenylamine (DPA) spot test**: Indicated nitrates are present in the overall substrate and repair. Repeated the test twice with the guidance of Lara Kaplan to confirm a positive result.
    - **Transmission FTIR**: Confirmed the substrate is cellulose nitrate (see "Appendix IV. Additional Analysis" for additional information). Completed testing with the guidance of Dr. Liora Mael.
    - **Silver nitrate[15] and sulfuric acid[16] spot tests**: Although the corrosion products on the ferrous repairs are similar in appearance to chloride corrosion on iron, the silver nitrate and sulfuric acid spot tests were negative. This indicates the corrosion is more likely initiated by nitrates from the offgassing cellulose nitrate substrate. Completed these spot tests with the guidance of Lauren Fair.
    - **Cross section microscopy (CSM)**: Although proposed, I did not revisit Amber Kehoe's CSM sample. The extent of crazing on internal and external surfaces, as well as potential layer structures, were more suitably investigated with microscopy.
3. **Mechanically reduced and stabilized corrosion products** (17 hours).
    - **Mechanical reduction**: I removed loose corrosion particles with a HEPA filtered low-speed vacuum with a narrow nozzle covered with cheesecloth. I removed loose corrosion particles with a brush and a HEPA-filtered variable-speed vacuum with a microtool attachment covered with cheesecloth. I then

---

[15] This spot test establishes the presence of chloride ions (Cl-) in corrosion products and other substances. Chloride ions are dissolved and acidified in a solution of nitric acid ($HNO_3$), then reacted with silver nitrate ($AgNO_3$) to form silver chloride (AgCl), a white precipitate (Odegaard, Carroll, and Zimmt 2000, 108).

[16] This spot test establishes the presence of chloride ions (Cl-) in inorganic compounds with sulfuric acid. Concentrated sulfuric acid ($H_2SO_4$) reacts with chloride salts to form volatile hydrogen chloride (HCl), which can be shown by the reaction with acid indicators on pH paper. (Odegaard, Carroll, and Zimmt 2000, 104).

reduced corrosion under magnification with an insect pin and scalpel (#11 blade). I applied Shellsol D-38[17] with a swab to penetrate corrosion layers and disrupt bonding forces to increase the effectiveness of mechanical action. I periodically cleared the corrosion with the vacuum and cosmetic sponges. I used silicone release Mylar templates to protect the cellulose nitrate. Once removed, the corrosion quickly returned, indicating the rate of corrosion is even more rapid in stable environmental conditions than previously hypothesized (fig. 22).

Figure 22. Before (left), immediately after (center), and two weeks after (right) mechanical corrosion reduction.

- **Stabilization**: A coating was necessary to slow the rate of corrosion, particularly on newly exposed surfaces. In two locations, I tested 10% (w/v) Paraloid B-48N[18] in acetone with 1% (w/v) dodecanethiol[19] as a corrosion inhibitor and 2% ethanol to increase the working time (table 2). The surface darkened and increased in gloss slightly, and texture was reduced but still visible. Aside from the glossiness, the coating improved the aesthetic legibility of the metal and successfully minimized the return of corrosion products. Adding a pinch of hydrophilic fumed silica[20] as a matting agent reduced the glossiness. I applied the coating to all exposed metal surfaces with careful attention to minimize acetone exposure to the substrate. In areas where excess gloss remained, I applied Cosmoloid H-80 microcrystalline wax[21] in Shellsol D-38 over the Paraloid B-48N.

Table 2. Coating tests following corrosion reduction of left staple only. 160x magnification.

| Location | Day 0 (before coating) | Day 0 (after coating) | Day 15 |
|---|---|---|---|
| PR, waistcoat, repair area second from the bottom. |  |  |  |

[17] A highly refined petroleum solvent with very low aromatic content and rather slow evaporation rate.
[18] Clear colorless thermoplastic acrylic resin composed of a methyl methacrylate/ butyl acrylate copolymer. Contains an adhesion promoter that assists bonding to bare and primed metals. Manufactured by Rohm & Haas and available from conservation suppliers.
[19] 1-Dodecanethiol (also known as lauryl mercaptan or n-dodecyl mercaptan) is a thiol compound (C12H26S) that can act as a corrosion inhibitor.
[20] Colloidal form of silica made by hydrogen-oxygen furnace combustion of silicon tetrachloride. This type is hydrophilic. Available from Conservation Emporium.
[21] Brand name for a hard microcrystalline wax used primarily as a protective coating on iron and other metals, and in varnishes to improve flow properties and sheen. Its reported melting temperature is 166-176F. Different from other traditionally used microcrystalline waxes such as Renaissance wax, which are blends, Cosmoloid H 80 is a pure wax and has been proven to have comparably better reversibility (Moffett, D.L., "Wax Coatings on Ethnographic Metal Objects: Justifications for Allowing a Tradition to Wane," In JAIC 1996, Vol. 35, No. 1, Article 1, pp. 1-7). Available from Kremer Pigments.

| | |
|---|---|
| PR neck | 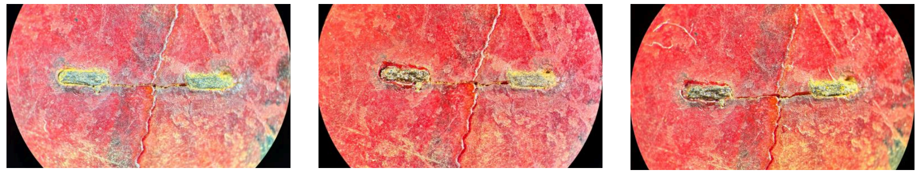 |

- I left one staple on the PR shoulder with only the Paraloid B-48N and no additional wax for long-term evaluation of the impact of coatings on corrosion formation for this particular object (fig. 23).

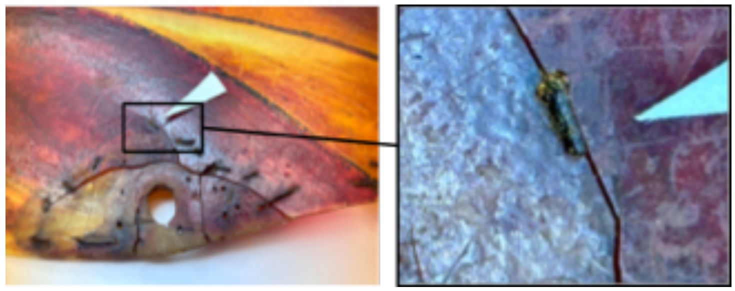

Figure 23. Location of staple with Paraloid B-48N coating only.

4. **Cleaned surface overall** (*2 hours*).
    - I reduced remaining corrosion products and surface grime with a cosmetic sponge and HEPA-filtered vacuum in linear passes (fig. 24). In the most degraded areas of the substrate near the leg loss and areas of flaking red colorant, surface cleaning was not possible.

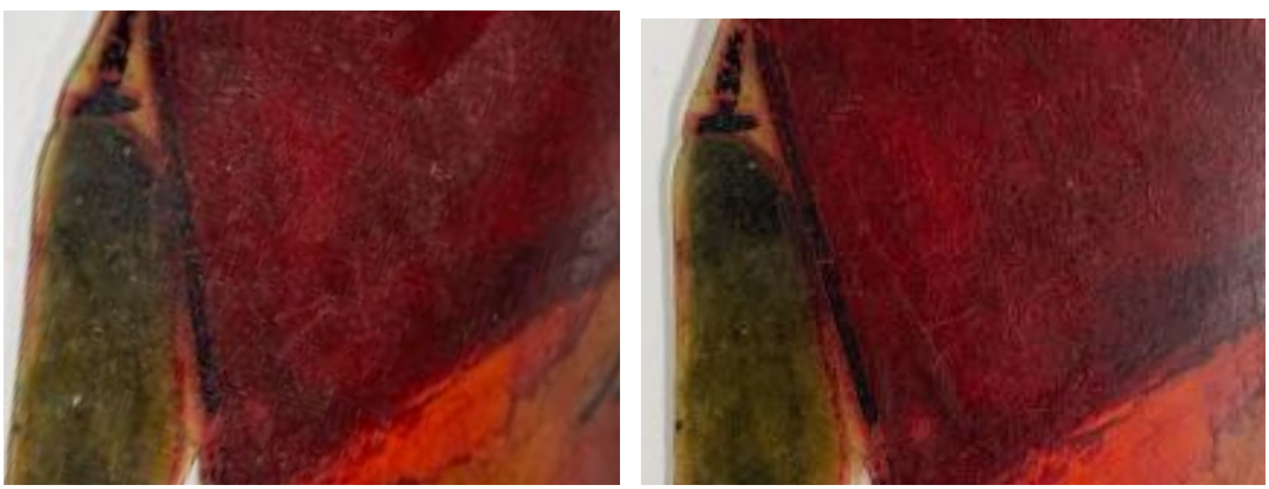

Figure 24. Before (left) with a single cleaning test in the upper center and after (right) surface cleaning the fez.

5. **Reduced surface blooms** (1.5 hours).

    - The slightly rough, hazy appearance (previously attributed to a surface bloom) of the PR face, upper cape, and lower cape disappeared when solvent testing with Shellsol D-38. However, when the solvent evaporated, the haziness returned. This indicated that the condition was due to localized micro-cracks rather than a surface deposit. Addressing these areas with consolidation was therefore more appropriate than solvent cleaning or mechanical action.

    - I successfully removed small white surface deposits on the PR leg, near the upper component with gentle mechanical action under magnification (fig. 25). Touching the bloom with the tip of an insect pin provided enough pressure to dislodge the deposits.

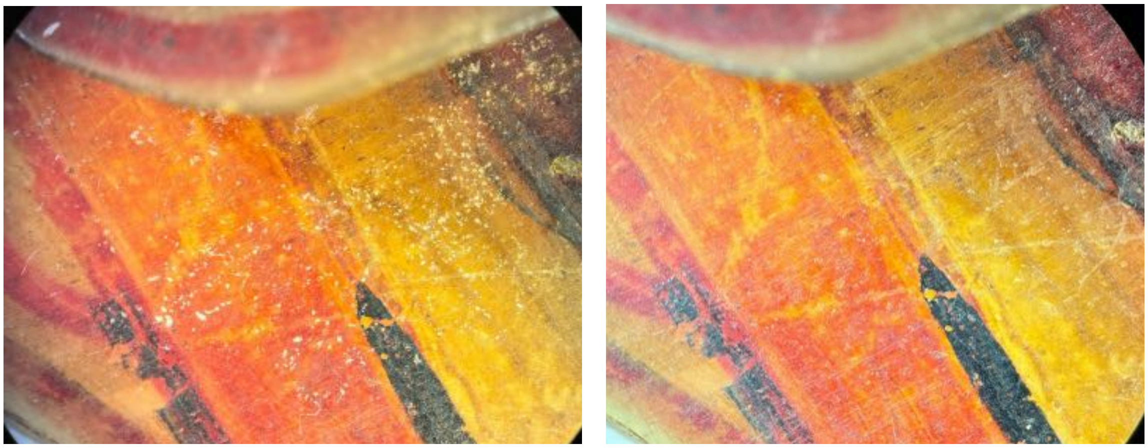

Figure 25. Before (left) and after (right) reducing surface deposits on the upper PR of the leg component.

- I applied slightly excessive pressure in removing a surface accretion on the center lower cape and unintentionally removed the underlying colorant along with it. Under magnification (fig. 26), this change is very notable. From a distance, it is visible but does not stand out among the surface irregularities already present (fig. 27). This created an opportunity to reflect on the importance of continuously evaluating the extent of treatment, remaining aware of the balance required to avoid pushing treatment too far or not far enough. The accretion attracted significant hygroscopic dust, which may have accelerated the substrate degradation over time. However, its removal was not essential for the preservation of the object and in hindsight, leaving it alone would have been better.

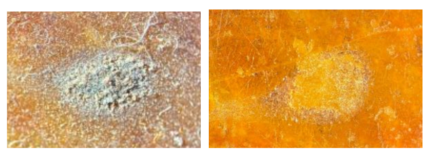

Figure 26. Before (left) and after (right) surface cleaning and removing surface accretion. Lighting conditions vary.

Figure 27. Overall view, removed accretion indicated with white arrow.

6. **Consolidated areas of severe embrittlement and cubic crystal formation** (*15 hours*).

   - I completed solubility testing, evaluating the impact on the red colorant and the substrate (table 3). I selected deionized water, n-butanol, Shellsol D-38, and Shellsol T[22] for further consolidant tests since they penetrated well and induced the fewest changes in condition (table 4). 5% Paraloid B-67[23] in Shellsol D-38 with 0.5% xylene (w/v) penetrated most effectively with minimal changes in gloss, so I used it for consolidation.

Table 3. Solubility testing results.

| Solvent | Red colorant | Substrate after 48 hours |
|---|---|---|
| Isopropanol | Slightly soluble | Substrate slightly dissolved, significant material displacement |
| Ethanol | Very soluble | Substrate completely dissolved, hazing, significant material displacement |
| 1:1 isopropanol and ethanol | Slightly soluble | Substrate completely dissolved, significant displacement |
| DI water | Not soluble | Substrate slightly dissolved, minimal displacement |
| n-butanol | Slightly soluble, movement of colorant | No effect |
| Low aromaticity mineral spirits (Shellsol D-38) | Slightly soluble, but no movement of colorant unless disturbed | No effect |
| *Shellsol D-38 w/ 0.5% xylene* | Slightly soluble, but no movement of colorant unless disturbed | No effect |
| 1:1 DI water and isopropanol | No change | White hazing on one edge, no dissolving of substrate |
| Shellsol T (Aspiration hazard category 1 ) | No change | No change |

Table 4. Consolidant testing results.

| Consolidant | Before | During | After | Notes |
|---|---|---|---|---|
| 5% Aquazol 500[24] in DI water (w/v) |  |  |  | Increase in gloss, reduction in visible internal crizzling, somewhat limited penetration |

[22] A synthetic isoparaffinic hydrocarbon solvent with very low aromatic content. Sold by Kremer Pigments.
[23] Clear colorless thermoplastic acrylic resin composed of isobutyl methacrylate. Previously manufactured by Rohm & Haas, now produced by The Dow Chemical Co. and available from conservation suppliers.
[24] Adhesive composed of poly(2-ethyl-2-oxazoline); soluble in water and polar organic solvents (acetone, ethanol, etc.); molecular weight = 500,000; kinematic viscosity=60-80 cSt. Manufactured by Polymer Chemistry Innovations; available from conservation suppliers.

| | | | | |
|---|---|---|---|---|
| 5% Aquazol 200[25] in DI water (w/v) | 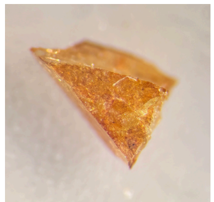 | 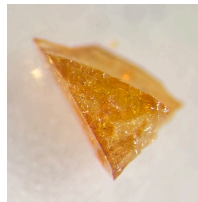 |  | Slight increase in gloss, slight reduction in surface texture, greater penetration |
| 5% Paraloid B-67 in n-butanol (w/v) | 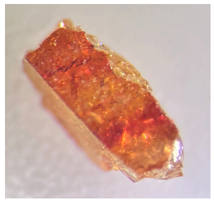 | 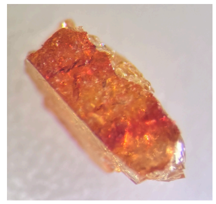 |  | Penetrated a lot, too shiny |
| 5% Plexigum PQ611[26] in Shellsol T (w/v) | 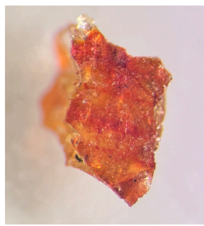 | 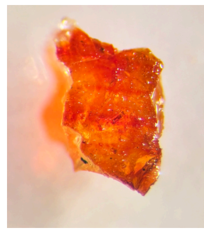 | 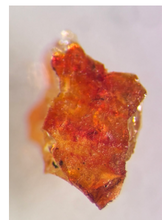 | Penetrated a lot, very slight shine, most surface texture maintained |
| 5% Paraloid B-67 in Shellsol D-38 with 0.5% xylene (w/v) |  |  |  | Penetrated a lot, no change in surface gloss |

- I consolidated degraded regions and areas immediately surrounding staple repairs with the 5% Paraloid B-67 in Shellsol D-38 with 0.5% xylene (w/v) following testing (fig. 28-29). Surface gloss continuity was greatly improved.

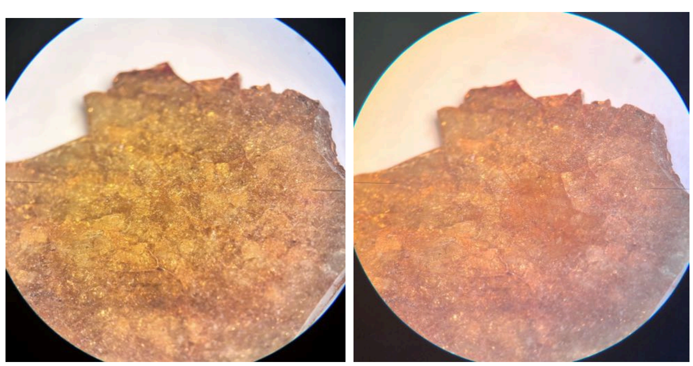

Figure 28. Before (left) and after (right) consolidation. Lighting conditions vary slightly.

[25] Adhesive composed of poly(2-ethyl-2-oxazoline); soluble in water and polar organic solvents (acetone, ethanol, etc.); molecular weight = 200,000; kinematic viscosity = 18-24 cSt. Manufactured by Polymer Chemistry Innovations. Available from conservation suppliers.

[26] Isobutyl methacrylate-based resin, also known as Degalan PQ 611; soluble in esters, ketones, aromatic hydrocarbons, and aromatic-free aliphatic hydrocarbons (e.g. Shellsol T); insoluble in alcohols. Sold by Kremer Pigments.

Figure 29. Consolidation locations indicated with green.

7. **Applied a localized facing to further stabilize embrittlement** *(3 hours)***.**

    - Prior to flipping the puppet over, I applied a temporary facing with HM-3 Mino Gampi[27] mulberry paper with 10% Paraloid B-67 in Shellsol D-38 with 0.5% xylene, following reversibility testing with Shellsol D-38. Once stabilized with a facing, the legs of the puppet were rotated slightly counterclockwise to align with the painted edge of the upper puppet component (fig. 30).

[27] Strong, stable hand- or machine-made papers made of long bast fibers (e.g. paper mulberry). Comes in several thicknesses, opacities, fiber types and lengths, etc. Available from Hiromi Paper, Inc. (http://store.hiromipaper.com/) or conservation suppliers.

Figure 30. Temporary facing to support embrittled fragments while flipping the puppet over (left). The new leg orientation, aligned with the painted edges of the upper component (right).

8. **Flipped the puppet to address condition issues on verso** (*7 hours*).

   - Lara Kaplan and I created a temporary support system (with Ethafoam,[28] Volara foam,[29] polyester batting, Tyvek,[30] and Hollytex[31] attached with 3-M double-sided tape[32]) to pad the puppet and ensure it would not be crushed when flipped (figs. 31-32).

Figure 31. Layers of support to prepare for flipping the puppet over.

---

[28] Closed-cell, low density polyethylene foam made by injecting halogenated gas (dichlorodifluoromethane) into the polymer melt. Some products may contain stearyl stearamide (1%) as a slip agent, as well as trace amounts of antioxidants and UV absorbers. Manufactured by Dow Chemical Co.

[29] Closed cell plastic foam made from polyethylene. It has a smooth surface that is resistant to water absorption and chemical reactions. Made in various thicknesses and colors. Manufactured by Voltek. Available from conservation and plastics suppliers.

[30] Spunbonded olefin fabric, 100% high density polyethylene with no fillers or binders. It has fine, white, continuous filaments that are bonded by heat and pressure. Manufactured by DuPont.

[31] Fabric made of white spun-bonded nonwoven polyester fibers calendared to a smooth surface. Available in a variety of thicknesses. Commonly used as a support material, interleaving paper, or backing. Reemay® (Reemay, Inc) is a similar product. Available from conservation suppliers.

[32] A thin polymer or paper strip with pressure-sensitive adhesive on both the upper and lower surfaces. The adhesive is 3M Acrylic Adhesive 400, the carrier is polyester terephthalate, and the liner is 60# densified kraft paper.

Figure 32. The verso of the puppet, prior to applying a lining.

- Once flipped, I performed the following treatment steps with the aforementioned methods: corrosion reduction, metal coating, surface cleaning, bloom reduction. Following testing, I applied a lining of untoned HM-1 Tengucho paper with 10% Paraloid B-67 in Shellsol D-38 with 0.5% xylene to the loss in the lower leg component. Once the treatment of the verso was complete, I flipped the puppet back over to the recto with the aforementioned supports.

9. **Reattached extant fragments** (*8 hours*).

   - I reattached fragments with 30% Paraloid B-67 in Shellsol D-38 with 0.5% xylene. I applied HM-1 Tengucho paper toned with Golden Fluid Acrylic[33] paints along break edges and vulnerable areas for increased structural support and aesthetic integration (fig. 33)

Figure 33. Fragments reattached.

[33] Lightfast, low-viscosity acrylic paints with a high pigment load. Manufactured by Golden Artist Colors; available at art stores and from Golden Artist Colors.

- I determined that select fragments belonged to puppets GACP 1995C and GACP 1595D based on color, translucency, and thickness. I moved these fragments to the housing enclosures of their associated puppets (fig. 34). I sorted the remaining small fragments by size into two bags, which will remain associated with the puppet (fig. 35).

Figure 34. Fragments associated with puppet: GACP 1995C (left) and GACP 1995D (right).


Figure 35. Fragments associated with GACP 1995A shadow puppet.

10. **Filled the large loss on the leg** (*3 hours*).

- I created HM-3 Mino Gampi detachable inserts toned with Golden Fluid Acrylics for aesthetic integration, following testing (fig. 36). I tested Vivak[34] fills toned with Golden Fluid Acrylics, which had well-matched thickness and transparency, but were not suited to match the highly angular edges of the loss. I also tested toned nanocellulose, but the material was too brittle for safe handling at this size.

Figure 36. Paper fill.

[34] Transparent, thermoplastic sheet composed of polyethylene terephtalate glycol-modified (PETG). Can be formed by break forming, cold bending, or with heat; bonded with adhesives, ultrasonic welding, or rivets; painted, silk-screened, or hot stamped. Not UV stabilized. Manufactured by U.S. Plastic Corporation.

11. **Applied an accession number** (*1 hour*).

    - I printed the accession number (size 8 calibri font) on Mellinex[35] with an inkjet printer and attached the label with 30% Paraloid B-67 in Shellsol D-38 with 0.5% xylene (w/v) in a discrete, but visually apparent location on the puppet recto (fig. 37).

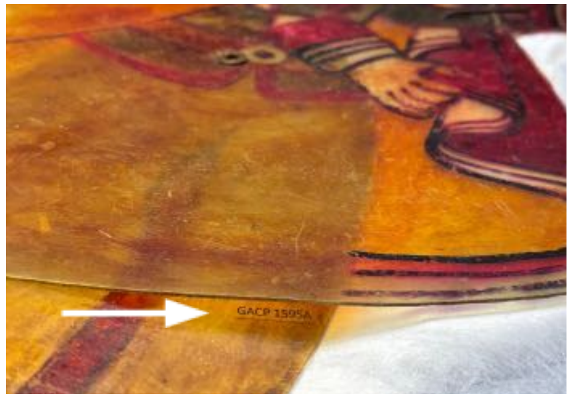

Figure 37. Accession number, only visible at a low angle under the top component.

12. **Updated the housing enclosure** (*4 hours*).

    - I updated the housing enclosure to minimize stress on the warped substrate with Volara supports covered with Tyvek and Hollytex to maintain a support surface with a low snag risk (fig. 38). The design maximized accessibility by creating a removable inner support for lifting the puppet. I used Lignin-Free Archival Board (or "blueboard")[36] as housing material since it adsorbs acidic by-products with minimal acceleration of plasticizer leaching (Coughlin 2023). The design maintained ventilation by creating an open housing enclosure with no lid to prevent the buildup of acidic gasses.

Figure 38. Housing enclosure (left) and removable component for handling (right).

[35] Translucent polyester film manufactured as part of the Mylar Specialty Films (formerly DuPont Teijin Films) market offering.
[36] Corrugated board made from bleached, lignin-free, alpha-cellulose pulp. It is required to be between a pH of 8.5-10.2, and contain alkaline sizing and an alkaline reserve (e.g. 3% calcium carbonate). Available from Conservation Resources.

- I trimmed cresol red indicator strips[37] from the prior housing enclosure at the edges, as the strips had just barely started to turn red only at the edges.

13. **Consider approaches to preserve the performance dimension of the puppet** *(4 hours).*

    - **Recreation:** To provide a reference as to the kinetic aspect of the puppet, I created a recreation of the puppet by applying a large sticker sheet with a photoshopped image of the before treatment documentation onto a sheet of polymethyl methacrylate (PMMA) (fig. 39). I then used a jewelers saw to cut out the two components, drill a hole, and join them with a rivet. If someone were to pursue an improved version of this recreation, a clear sticker (rather than one with a white backing as was used in this version) would more closely match the original puppet. Additionally, the after treatment photo documentation could be used as a reference. It may be worth testing the suitability of Vivak[38] as a substrate, rather than PMMA, since the PMMA was difficult to cut crevices without creating small stress cracks.

Figure 39. Components of the recreation (left) and completed recreation (right). Right image courtesy Leah Palmer.

    - **Shadow documentation**: I was able to photograph the shadow of this puppet, with the guidance of Conservation and Collections Photographer Nat Caccamo. I used a copy stand imaging setup with a

[37] Indicator strips designed to detect volatile acidic components released by the decomposition of cellulose nitrate. These strips contain a pH sensitive dye (o-cresol-sulfonphthalein) that changes from yellow to red from pH 7.2 - 8.8.

[38] Transparent, thermoplastic sheet composed of polyethylene terephtalate glycol-modified (PETG). Can be formed by break forming, cold bending, or with heat; bonded with adhesives, ultrasonic welding, or rivets; painted, silk-screened, or hot stamped. Not UV stabilized. Manufactured by U.S. Plastic Corporation.

large-scale dimmable LED light pad underneath the puppet and a clean cotton sheet laid overtop.[39] The colors of the puppet were prominent in the shadow created, and the soft hazy outline of the puppet when it is used in performance can now be visualized (fig. 40). No photo documentation of this puppet's shadow was previously associated with the object.

[39] Documented with Nikon D800 device, Nikon D series 30 mm focal length, f/16, exposure 1/125. Post-processing included white balance adjustment to match the appearance of the object visually, -0.10 exposure, cropping, and brightening the region of the fill, as this area was more opaque and darker than the rest of the puppet.

Figure 40. Documentation of the shadow, recto, after treatment.

Figure 41. Documentation of the shadow, verso" after treatment.

14. **Carried out post-treatment photodocumentation and wrote treatment repor**t (*5 hours*)

**Total treatment time**: 78.5 hrs

### Environmental and Handling Recommendations

Ideally, this shadow puppet would benefit from cold storage (<68°F), if that becomes possible in the future. An anoxic environment would halt corrosion, but this will likely not be feasible. In general, 35-45% RH should be maintained, as >50% RH can accelerate hydrolysis of the substrate which releases nitric acid, and <25% RH can cause crazing. <50 lux and limited UV exposure will minimize cellulose nitrate photo-oxidation (Coughlin 2023). Light exposure should be minimized due to the light-sensitivity of the potential lake colorant.

**Treated By**: Daisy Diamond **Report Date:** May 9th, 2025

## References

Braun, Thomas J. "An Alternative Technique for Applying Accession Numbers to Museum Artifacts," *Journal of the American Institute for Conservation* 46, no. 2 (January 2007): 91–104, https://doi.org/10.1179/019713607806112323.

Bruyn-Ouboter, Vera and Hartmut Kutzke, "The Interaction between Musical Instrument Steel Strings and Cellulose Nitrate," *7th International Congress Chemistry for Cultural Heritage (ChemCH)*, 2024, 42–43.

Corona, M., Owens, S. 2016. "Comparing Cleaning Methods for Cellulose Nitrate: Study of the Silicone Solvent D4." In *The Shock of the New: Modern Materials, Media and Methods*. Joint Objects and Electron SIG Symposium. February 8 to 10 2017 – Melbourne Museum. Melbourne: Australian Institute for the Conservation of Cultural Material.

Coughlin, Mary. 2023. "Plastics" and "Plastics: Identification and Monitoring" PowerPoint presentation, Conservation Principles: Organic Block, Winterthur/University of Delaware Program in Art Conservation.

Derrick, Michele R., Dusan Stulik, and James M. Landry. 1999. *Infrared Spectroscopy in Conservation Science. Scientific Tools for Conservation.* Los Angeles, CA: Getty Conservation Institute. http://hdl.handle.net/10020/gci_pubs/infrared_spectroscopy

Dyer, Joanne and Nicola Newman. 2020. "Multispectral Imaging Techniques Applied to the Study of Romano-Egyptian Funerary Portraits at the British Museum." *Mummy Portraits of Roman Egypt: Emerging Research from the APPEAR Project.* Los Angeles, CA: J. Paul Getty Trust.

Fair, Lauren. 2024. "Metals Treatment" PowerPoint presentation, Conservation Principles: Inorganic Block, Winterthur/University of Delaware Program in Art Conservation.

Kakoulli, Ioanna et al., "Application of Forensic Photography for the Detection and Mapping of Egyptian Blue and Madder Lake in Hellenistic Polychrome Terracottas Based on Their Photophysical Properties," *Dyes and Pigments* 136 (January 2017): 104–15, https://doi.org/10.1016/j.dyepig.2016.08.030.

Selwyn, Lyndsie. 2004. *Metals and Corrosion: A Handbook for the Conservation Professional*. Ottawa, Ont: Canadian Conservation Institute.

Selwyn, Lyndsie, P J Sirois, and V Argyropoulos. 1999. "The Corrosion of Excavated Archaeological Iron with Details on Weeping and Akaganéite," *Studies in Conservation* 44, no. 4: 217–32.

Myrsiades, Linda S, and Kostas Myrsiades. 1992. *Karagiozis : Culture & Comedy in Greek Puppet Theater*. Lexington: University Press of Kentucky.

Papageorgiou, Ioanna. 2014. "The Mountain Bandits of the Hellenic Shadow Theatre of Karaghiozis: Criminals or Heroes?" *Popular Entertainment Studies 5,* no. 2: 79-102.

Reilly, J. A. 1991. Celluloid Objects: Their Chemistry and Preservation. Journal of the American Institute for Conservation 30 (2): 145-162. http://http://cool.conservation-us.org/jaic/articles/jaci30-02-003.html

Shashoua, Yvonne, Michael Schilling, and Joy Mazurek. "The Effectiveness of Conservation Adsorbents at Inhibiting Degradation of Cellulose Acetate." ICOM Committee for Conservation 17th Triennial Meeting Melbourne Australia. 2014.

Zimmt, Werner, Scott Carroll, and Nancy Odegaard. *Material Characterization Tests for Objects of Art and Archaeology*. 2nd ed. London: Archetype Publications, 2000.

# Appendix I: Before Treatment Photo Documentation

The front of the shadow puppet was photographed before treatment (fig. I-1). However, the object was too unstable to flip, and the back was not able to be documented.

Figure I-1. Overall recto before treatment, normal illumination.[40]

[40] Documented with Nikon D800 device, Nikon D series 60 mm focal length, f/16, exposure 1/125. Post-processing included white balance , -0.10 exposure, and cropping.

Under long-wave UV radiation, the red media emits a bright orange; the tassel of the fez, face, cape interior, shirt, and pants emit an inconsistent muted yellow-orange; and the substrate emits a light blue-green induced by ultraviolet excitation (fig. I-2). The bright orange fluorescence of the red could be attributed to the presence and spatial distribution of madder lake dyes or pigments. However, this is not conclusive due to similar fluorescence characteristics of other colorants, binders, or coatings (Kakoulli et al. 2017).

Figure I-2. Overall recto before treatment, ultraviolet induced visible luminescence (UVL).[41] Image captured in collaboration with Dr. Roxanne Radpour.

[41] Documented with Nikon D800 device, Nikon D series 60 mm focal length, f/11, exposure 8." Light wand painting with Model UVL-56 Blak-Ray® Lamp Long Wave UV - 365nm, 115V, 60 Hz, 0.16 amps. Post-processing included white balance (medium), exposure -0.50, and use of the stamp tool to remove significantly distracting marks from the black backdrop. Note: the object was too fragile to move, so black paper was placed around the object to reduce the impact of the bright fluorescence of the objects support.

Visible-induced visible luminescence (VIVL) images record the emission of light between 500–700 nm when the object is illuminated with 400–500 nm. This image is particularly useful for characterizing the spatial distribution of yellow and red lake pigments, such as madder (Dyer and Newman 2020). The red colorant is likely a madder-based dye due to the bright luminescence observed in VIVL that corresponds to areas of bright orange fluorescence in UVL (fig. I-3).[42]

Figure I-3. Recto detail image, visible induced visible luminescence (VIVL), before treatment. Image captured in collaboration with Dr. Roxanne Radpour.

[42] Documented with a modified Nikon D800 DSLR camera (low-pass filter ICF/AA removed), Nikon D series 60 mm focal length, f/11, 8” exposure. Light source: a party light with multiple color outputs. Post-processing included transformation to grayscale.

## Appendix II: After Treatment Photo Documentation

After treatment documentation included both sides of the puppet (fig. II-1 and II-2).[43]

Figure II-1. Overall recto after treatment, normal illumination.

[43] Documented with Nikon D800 device, Nikon D series 60 mm focal length, f/16, exposure 1/125. Post-processing included white balance , -0.10 exposure, and cropping.

Figure II-2. Overall verso after treatment, normal illumination.

# Appendix III. Prior Analysis

**Transmission-Fourier transform infrared spectroscopy (FTIR)**

Transmission-FTIR spectroscopy was performed on a small extant fragment with Dr. Kristin deGhetaldi in 2016 and determined to match cellulose nitrate and camphor plasticizer, due to the secondary peak at 1725 $cm^{-1}$ (figs. III-1 to III-2).[44]

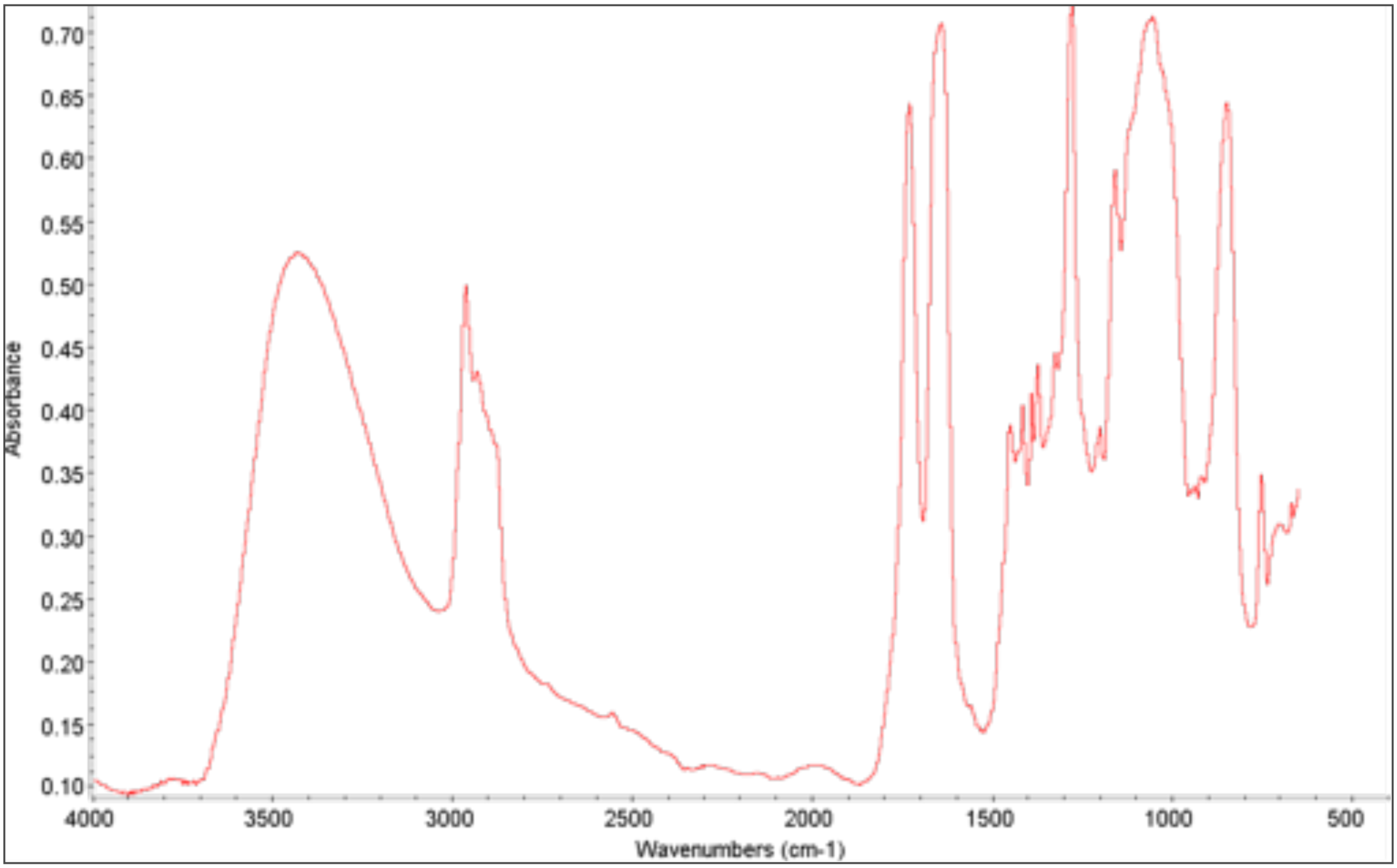


Figure III-1. GACP 1595A transmission FTIR spectrum collected by Dr. Kristin deGhetaldi and Amber Kehoe, November 2016.

[44] *Transmitted-FTIR spectroscopy with a diamond cell was performed on a small fragment crushed under magnification. The spectrum generated was compared to a database and the results were interpreted by Dr. DeGhetaldi and Dr. Petersen* (Kehoe 2016, 17).

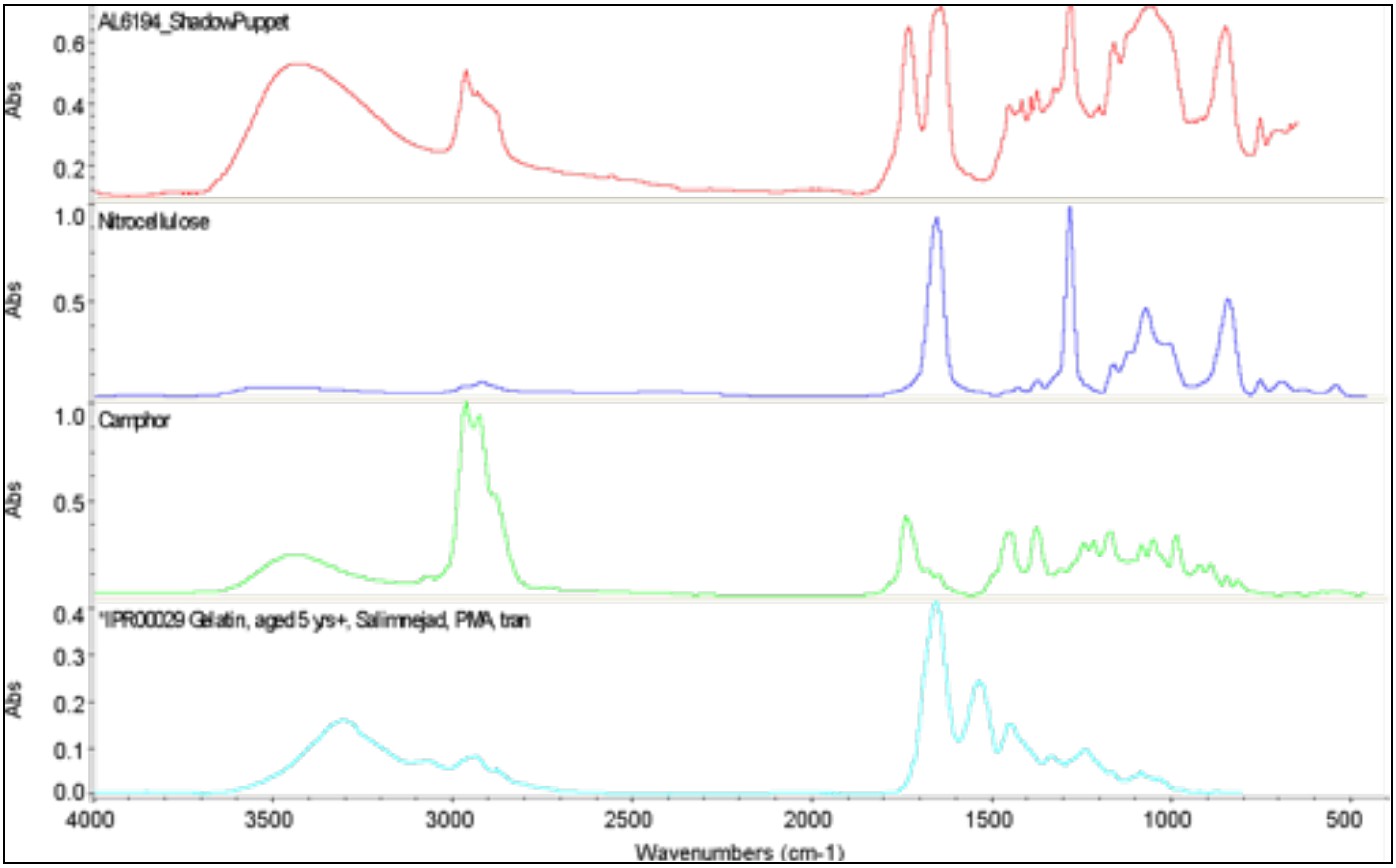


Figure III-2. FTIR spectra comparison - GACP 1595A, nitrocellulose, camphor, and aged gelatin. FTIR spectra source: Dr. Kristin deGhetaldi and Amber Kehoe, November 2016 and a reference spectral database.

**2. Portable X-ray fluorescence (XRF) spectroscopy**

XRF was performed on five locations of the shadow puppet (fig. III-3).[45] One spectra is included in this report as a representation: rhodium peaks are present as artifacts from the detector. Calcium may be present from surface dirt and paper board housing; iron may also be from surface dirt or corrosion products from the object itself; copper may be from surface dirt or copper-containing components of the XRF device; and zinc may be due to dirt on the surface, zinc oxide stabilizers in the polymer, or zinc-containing components of the XRF device. This indicates the paints and dyes are likely organic (Kehoe 2016, 18).

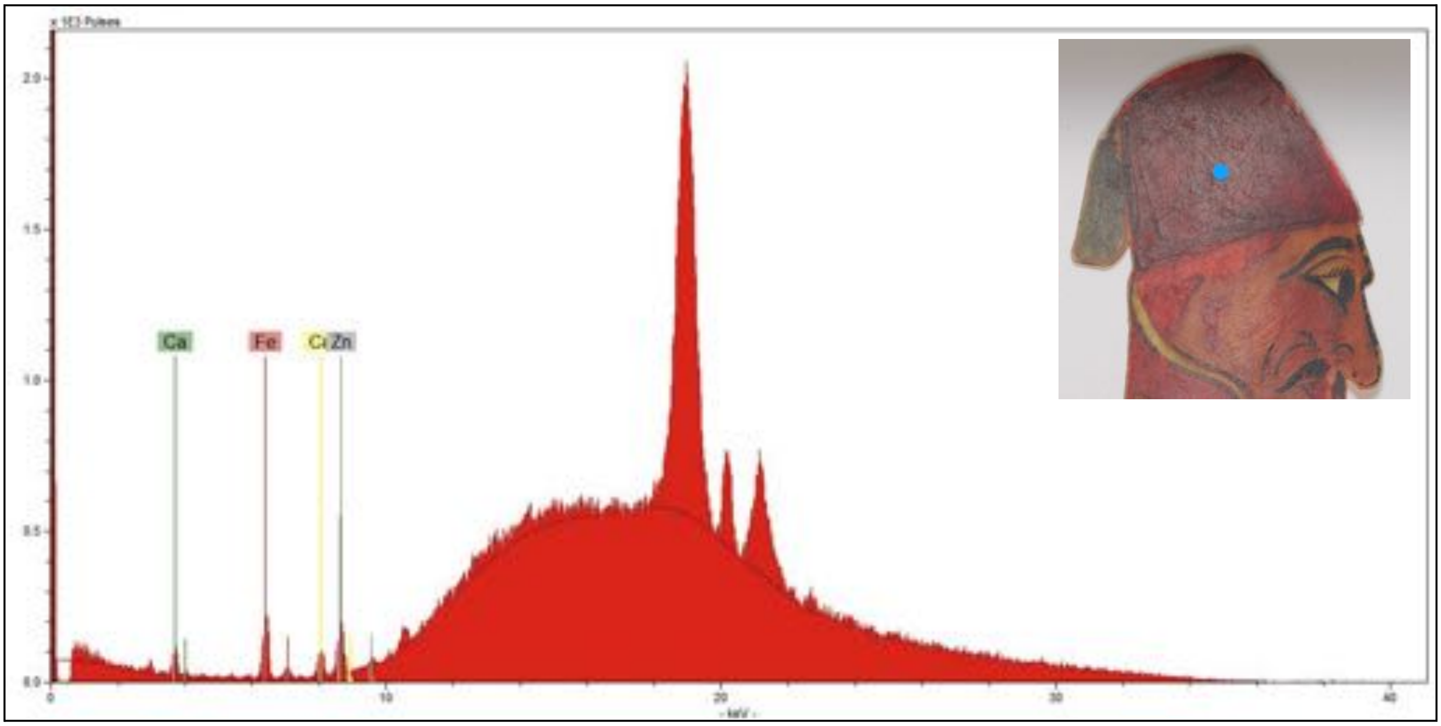


Figure III-3. XRF GACP 1595A; red fez. XRF spectrum courtesy Dr. Kristin deGhetaldi and Brian Baade, November 2016.

[45] Analysis was recorded as "performed with a handheld Bruker XRF at 40 kV, 9.6 µA" (Kehoe 2016, 18).

**3. Cross section microscopy (CSM)**

CSM was performed on a small extant fragment (figs. III-4 and III-5).[46] *Fluorescent paint/dye layers were visible on the top and bottom surfaces. The paint/dye appeared to migrate into the degraded areas of the substrate where cracking existed* (Kehoe 2016, 18). Within the interior of the substrate, irregularities were noted which could be inclusions, colorants, or simply air bubbles.

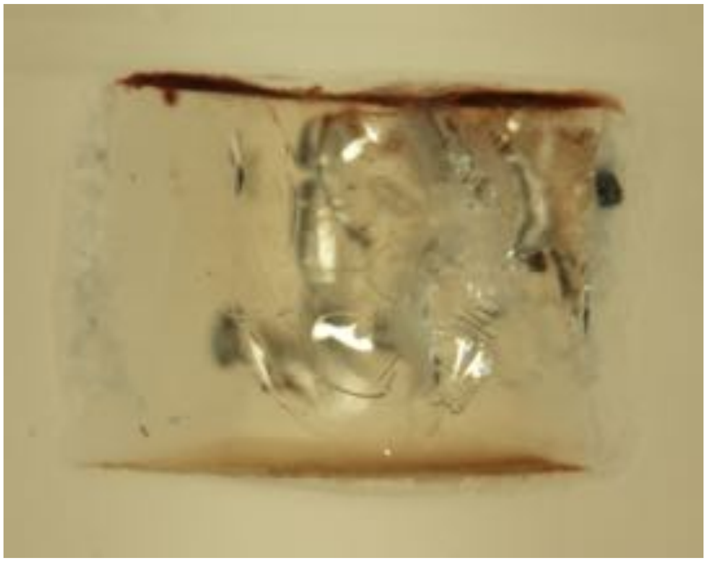

Figure III-4. Cross section GACP 1595A in visible light, 40x magnification. Image courtesy Matthew Cushman and Amber Kehoe, November 2016.

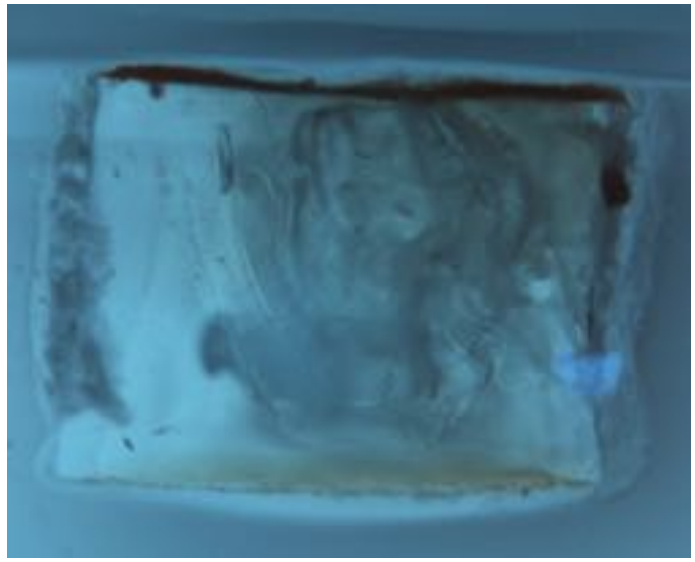

Figure III-5. Cross section GACP 1595A in UV radiation, 40x magnification. Image courtesy Matthew Cushman and Amber Kehoe, November 2016.

[46] *A small loss fragment was cast and polished in a polyester resin catalyzed with methyl-ethyl ketone peroxide (1% w/w) by Amber Kehoe under the guidance of Matthew Cushman* (Kehoe 2016, 18).

# Appendix IV. Additional Analysis

### Transmission Fourier Transform Infrared (FTIR) Spectroscopy

Two samples from fragments dissociated near the central loss to the legs were analyzed by transmission-FTIR microspectroscopy, an analytical technique that is useful in the characterization of both inorganic and organic materials including proteins, resins, and pigments. The samples were prepared by placing them individually on a diamond cell and rolled flat with a steel micro-roller to decrease thickness and increase transparency. The sample was analyzed using the Thermo Scientific Nicolet 6700 FT-IR with Nicolet Continuμm FT-IR microscope (transmission mode); data was acquired for 128 scans from 4000 to 650 $cm^{-1}$ at a spectral resolution of 4 $cm^{-1}$. Spectra were collected with Omnic 8.0 software and analyzed in this program with various infrared and Raman users group (IRUG) and commercial reference spectral libraries.

Based on characteristic IR absorption bands and comparison to spectral reference libraries, the sample was classified as cellulose nitrate (fig. IV-1). Characteristic IR absorption bands for cellulose nitrate include: a 3600-3200 $cm^{-1}$ O-H stretching band, 3100-2800 $cm^{-1}$ C-H stretching bands, a 1660-1625 $cm^{-1}$ N-O stretching band, a 1285-1270 $cm^{-1}$ N-O stretching band, 1480-1300 $cm^{-1}$ C-H bending band, 1300-900 $cm^{-1}$ C-O bending bands, and a 890-800 $cm^{-1}$ bending band (Derrick, Stulik, and Landry 1999, 190). Based on the comparison of the spectra of the two fragments, the molecular degradation may have resulted in varied spectral responses, potentially indicating the variable extent of degradation within the substrate (fig. IV-2). However, additional research into the changes in FTIR caused by the degradation of cellulose nitrate would be required to further investigate this hypothesis.

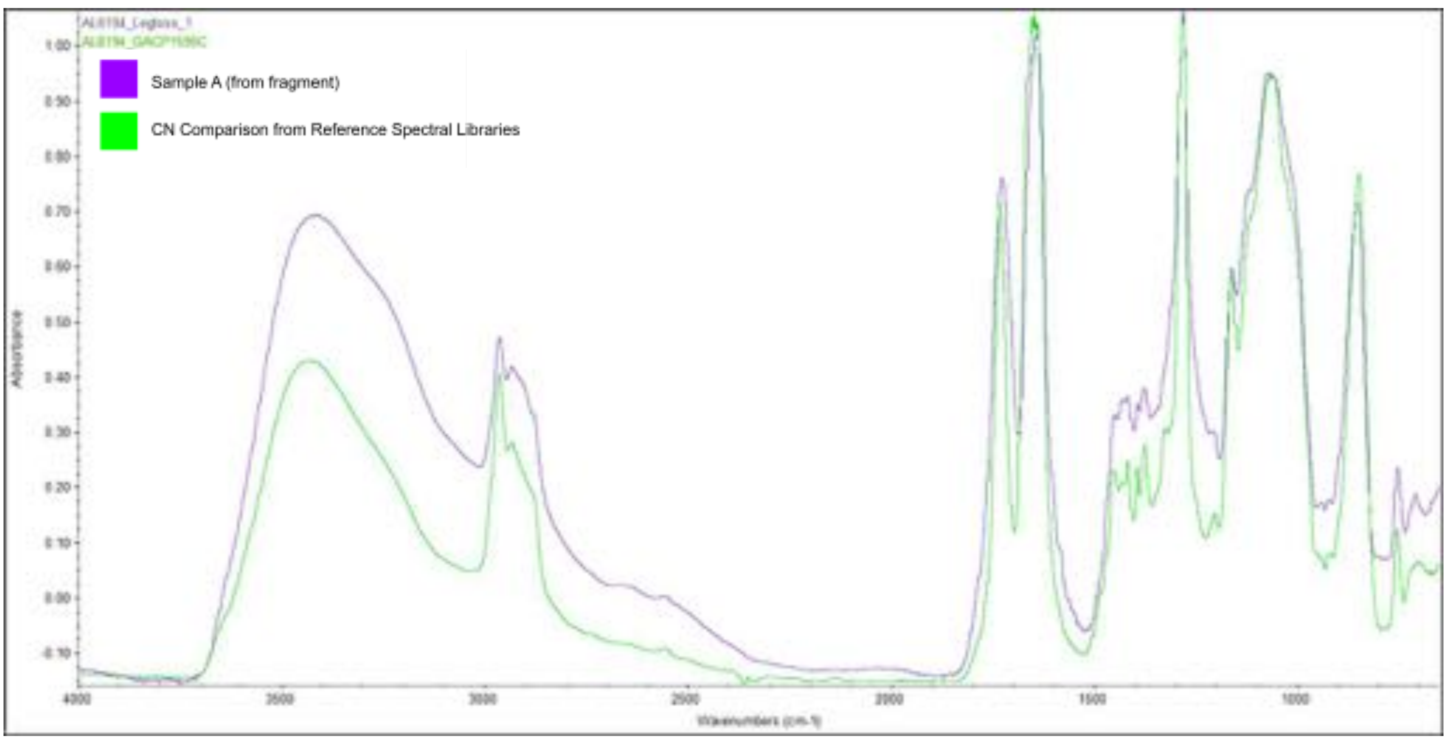


Figure IV-1. FTIR spectra comparison between GACP 1595A fragment and cellulose nitrate reference. FTIR spectra collected with Dr. Liora Mael, October 2024.

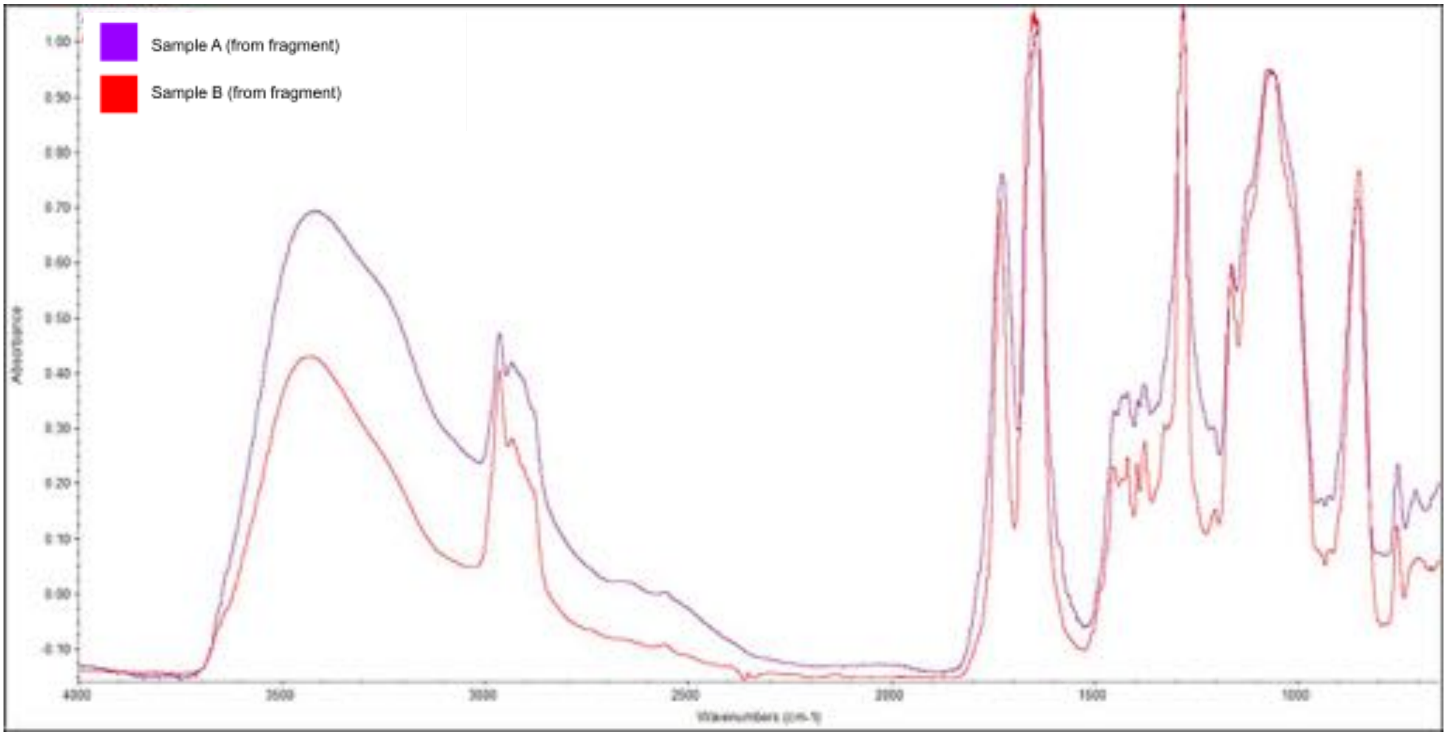


Figure IV-2. FTIR spectra comparison between two fragments collected for GACP 1595A. FTIR spectra collected with Dr. Liora Mael, October 2024.